VIP Cluster Compounds Very Important Paper

Deutsche Ausgabe: DOI: 10.1002/ange.201600275
Internationale Ausgabe: DOI: 10.1002/anie.201600275

Stability of $B_{12}(CN)_{12}^{2-}$: Implications for Lithium and Magnesium Ion Batteries

Hongmin Zhao[+], Jian Zhou[+], and Puru Jena**

Abstract: *Multiply charged negative ions are seldom stable in the gas phase. Electrostatic repulsion leads either to autodetachment of electrons or fragmentation of the parent ion. With a binding energy of the second electron at 0.9 eV, $B_{12}H_{12}^{2-}$ is a classic example of a stable dianion. It is shown here that ligand substitution can lead to unusually stable multiply charged anions. For example, dodecacyanododecaborate, $B_{12}(CN)_{12}^{2-}$, created by substituting H by CN is found to be highly stable with the second electron bound by 5.3 eV, which is six times larger than that in the $B_{12}H_{12}^{2-}$. Equally important is the observation that $CB_{11}(CN)_{12}^{2-}$, which contains one electron more than needed to satisfy the Wade-Mingos rule, is also stable with its second electron bound by 1.1 eV, while $CB_{11}H_{12}^{2-}$ is unstable. The ability to stabilize multiply charged anions in the gas phase by ligand manipulation opens a new door for multiply charged species with potential applications as halogen-free electrolytes in ion batteries.*

The study of multiply charged molecular ions has a long history because of their importance in fundamental interstellar chemistry as well as in coordination chemistry. Stabilized by the presence of charge-compensating counter ions, multiply charged negative ions primarily exist in solution or as crystals, such as Zintl-phase compounds.[1,2] However, it is difficult to stabilize these species in the gas phase because of electrostatic repulsion between the excess charges.[3] This aspect is particularly true for small multiply charged anions which either loose electrons (auto-detachment) or fragment without encountering significant energy barriers. Thus, finding ways to stabilize multiply charged ions in the gas phase is a long-standing challenge.[4,5]

One classic example of a multiply charged dianion which is stable in the gas phase is the icosahedral $B_{12}H_{12}^{2-}$ molecule, wherein the binding energy of the first (second) electron is 4.6 eV (0.9 eV).[6,7] The stability of the $B_{12}H_{12}^{2-}$ cage is governed by the Wade-Mingos rule.[8–11] According to this rule, $(n+1)$ pairs of electrons are necessary for cage bonding where n is the number of vertices on the boron icosahedral cage. It has recently been shown that highly stable dianions forming a sandwich complex can also be created in the gas phase by simultaneously satisfying multiple electron counting rules. For example, a multidecker $Cr[BC_5(CN)_6]_2^{2-}$ organometallic complex, which simultaneously satisfies the octet rule (of CN moiety), aromatic Hückle's rule (of organic BC_5 moiety), and 18-electron rule (of Cr atom), is very stable with the second electron bound by 2.58 eV.[12] A previous theoretical study also showed that TeF_8^{2-} is a very stable dianion with the second electron bound by about 5 eV.[13]

Here, we propose that ligand manipulation can lead to unusually stable dianions having an icosahedral cage structure. The importance of ligand engineering in stabilizing a monoanion has already been demonstrated in the case of benzene (C_6H_6). Replacing the ligand H by either F or CN increases the electron affinity (EA) of C_6H_6 from −1.15 eV to 0.75 eV in C_6F_6 and to 3.53 eV in $C_6(CN)_6$.[14] In this paper we consider *closo*-borane $B_{12}H_{12}^{2-}$ as an exemplary system. We note that a previous study has shown that substitution of H in $B_{12}H_{12}^{2-}$ by halogens (F, Cl, Br, and I) can increase the stability of dianion.[15] Herein we show that replacement of H with CN can lead to halogen-free $B_{12}(CN)_{12}^{2-}$ with great stability. The binding energy of the second electron in $B_{12}(CN)_{12}^{2-}$ is 5.3 eV, which is about a factor of six larger than the corresponding binding energy in $B_{12}H_{12}^{2-}$. To the best of our knowledge, no other molecule exists whose stability as a dianion is as high as that of $B_{12}(CN)_{12}^{2-}$. We also show another unusual property resulting from ligand engineering. Consider $CB_{11}H_{12}$, the carborane. This molecule needs only one extra electron to satisfy the Wade-Mingos rule.[8–11] Consequently, the EA of $CB_{11}H_{12}$ should be high. Indeed, a previous study found that its EA is 5.39 eV,[16] which is higher than that of any halogen atom. Hence $CB_{11}H_{12}$ is a superhalogen. When a second electron is added, $CB_{11}H_{12}^{2-}$ becomes unstable as it no longer satisfies the Wade-Mingos rule. We find that $CB_{11}(CN)_{12}^{2-}$, which is isoelectronic with $CB_{11}H_{12}^{2-}$ is more stable than its monoanion by as much as +1.07 eV. This stability further demonstrates the power of ligand engineering. We show that these unusual results can have technological applications in the design of halogen-free electrolytes in Li/Na/Mg ion batteries with improved performance.

To obtain the equilibrium geometries of $B_{12}(CN)_{12}$ molecules it was a priori not clear whether CN would bind to B with its C or N atom. Therefore, we optimized the structures by taking into consideration both possibilities. We found that $B_{12}(CN)_{12}$ with N atoms bound to B atoms is 5.48 eV higher in energy than the structure wherein C atoms are bound to B atoms. We also considered the possibility where the CN ligands attached to adjoining B atoms may buckle and dimerize. Following relaxation, the CN ligands did not dimerize and pointed radially outward. In Figure 1 a–c we show the optimized geometries corresponding to the lowest

[*] Prof. H. Zhao[+]
Department of Physics, School of Science
Beijing Jiaotong University (China)
Prof. H. Zhao,[+] Dr. J. Zhou,[+] Prof. P. Jena
Physics Department, Virginia Commonwealth University (USA)
E-mail: jzhou2@vcu.edu
pjena@vcu.edu
[+] These authors contributed equally to this work.

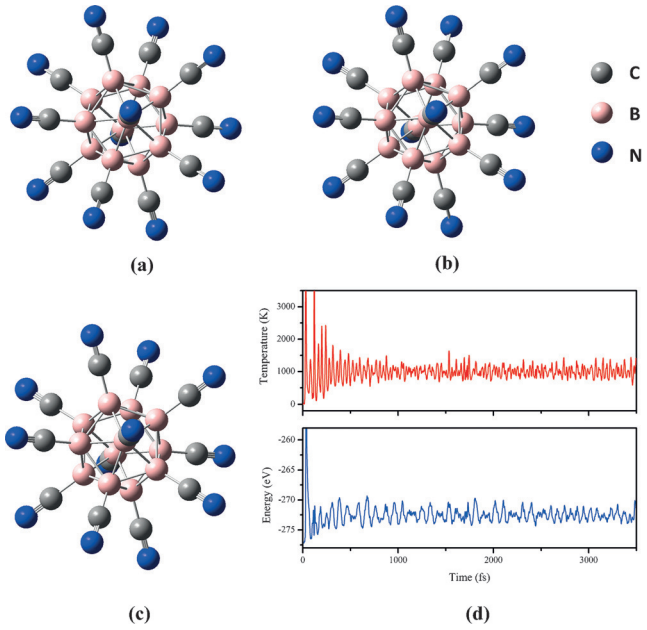

Figure 1. Geometric structure of a) neutral, b) monoanionic, and c) dianionic $B_{12}(CN)_{12}$. d) Total energy and temperature fluctuation, with respect to time, of an AIMD simulation of $B_{12}(CN)_{12}^{2-}$.

energy isomers of the neutral monoanion and dianion of $B_{12}(CN)_{12}$. The ground state of neutral $B_{12}(CN)_{12}$ has a D_{3d} point-group symmetry with average B–B, B–C, and C–N bond lengths of 1.79, 1.52, and 1.17 Å, respectively. The symmetry increases to T_d (I_h) when the first (second) electron is attached. The average B–B, B–C, and C–N bond lengths of $B_{12}(CN)_{12}^{2-}$ are 1.80, 1.54, and 1.16 Å, respectively. Note that the charged state of $B_{12}(CN)_{12}$ has minimal effect on these bond lengths. The binding energies of the first and second electron, calculated using both Gaussian 03 and VASP codes, are given in Table 1. These energies are defined as,

$$\Delta E_1 = E(X) - E(X^-) \quad (1)$$

$$\Delta E_2 = E(X^-) - E(X^{2-}). \quad (2)$$

Here X represents the molecule in question [$B_{12}(CN)_{12}$ or ($B_{12}H_{12}$)]. Note that the binding energies calculated using both the real space (Gaussian 03) and reciprocal space (VASP) approaches agree well with each other. Consequently, for the remainder of the calculations and discussions we only present results obtained using the Gaussian 03 code. The binding energy of the first electron, ΔE_1 for $B_{12}(CN)_{12}$, is almost twice that of $B_{12}H_{12}$, while ΔE_2 for the second electron (5.28 eV for $B_{12}(CN)_{12}$) is six times as large (0.86 eV for $B_{12}H_{12}$). We attribute this enhancement of binding energies in

Table 1: The binding energies (in eV) of the first and second electron of the studied dianions.

	$B_{12}H_{12}$	$B_{12}(CN)_{12}$	CB_{11} $(CN)_{12}$
ΔE_1 (G03/VASP)	4.57/4.68	8.56/8.77	8.72/8.90
ΔE_2 (G03/VASP)	0.86/0.97	5.28/5.51	1.07/1.29

$B_{12}(CN)_{12}^{2-}$ to two reasons: First, the electron affinity of the CN ligand is 3.86 eV, which is much larger than that of H (0.75 eV). The second reason is the size effect. As the size of the molecule increases, the electrostatic repulsion between excess charges decreases, hence enhancing the stability of the larger dianion. We define the diameter (d) of I_h $B_{12}(CN)_{12}^{2-}$ (and $B_{12}H_{12}^{2-}$) as the distance between the two opposite N (and H) atoms. The diameter of $B_{12}(CN)_{12}^{2-}$ is 8.83 Å which is larger than that of $B_{12}H_{12}^{2-}$ (5.81 Å).

To check its thermodynamic stability, we also performed ab initio molecular dynamics (AIMD) simulation using the Nosé-Hoover heat bath scheme[17] with the average temperature of the system at 1000 K. Time step is set to 1 femtosecond. After 3500 simulation steps (3.5 picoseconds), the $B_{12}(CN)_{12}^{2-}$ only exhibits slight distortions and can be optimized to its ground state at 0 K, thus establishing its thermodynamic stability (Figure 1 d).

According to our NBO analysis, in the neutral $B_{12}(CN)_{12}$, each CN receives 0.04 electrons on average from the B cage, and is consistent with the electronegative character of CN. The average valence electron configuration of each B, C, and N are $2s^{0.58}2p^{2.36}$, $2s^{0.92}2p^{2.93}$, and $2s^{1.60}2p^{3.52}$, respectively. To explore the nature of the excess electron distribution we calculated the electron deformation density of $B_{12}(CN)_{12}$ between different charged states (Figure 2 a and b). Green

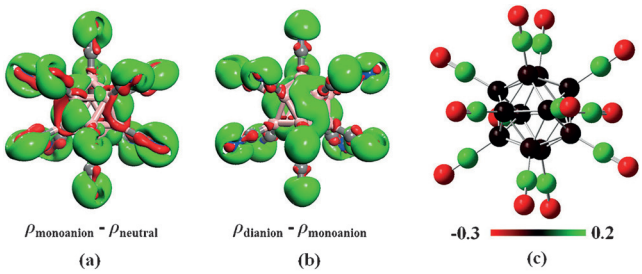

Figure 2. a,b) Electron densities in isosurface mode (0.005 | e | Å^{-3}). Green (light) and red (dark) colors represent positive and negative values, respectively. c) NBO charge distribution of $B_{12}(CN)_{12}^{2-}$.

and red colors represent electron accumulation and depletion regions, respectively. We observe that from the neutral state to monoanion, and from monoanion to dianion, the excess electrons distribute primarily on the CN ligands. To be specific, when forming the monoanion $B_{12}(CN)_{12}^-$, the α-spin electron configuration of each B, C, and N is $2s^{0.28}2p^{1.22}$, $2s^{0.46}2p^{1.45}$, and $2s^{0.80}2p^{1.83}$, respectively, while the corresponding electron configurations of β-spin are $2s^{0.28}2p^{1.18}$, $2s^{0.46}2p^{1.45}$, and $2s^{0.80}2p^{1.78}$, respectively. This data means that each CN pair receives about 0.08 electrons on average, and the B cage obtains about 0.02 electrons. When the second electron is attached, the electron configurations of each B, C, and N are $2s^{0.56}2p^{2.44}$, $2s^{0.92}2p^{2.86}$, and $2s^{1.59}2p^{3.70}$, respectively, thus suggesting that each CN pair and B atom gain about 0.13 and 0.03 electrons, respectively, on average. The larger electron gain on CN is consistent with its high electronegativity. The NBO charge distribution of $B_{12}(CN)_{12}^{2-}$ is given in Figure 2 c.

The electronic structure of $B_{12}(CN)_{12}^{2-}$ is further explored by calculating its energy level (Figure 3). The highest

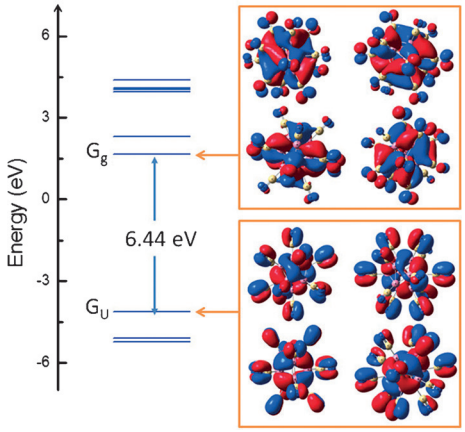

Figure 3. Energy diagram and frontier orbitals of $B_{12}(CN)_{12}^{2-}$.

occupied molecular orbital (HOMO) and lowest unoccupied molecular orbital (LUMO) are both fourfold degenerate with G_u and G_g symmetry, respectively. The HOMO–LUMO gap is estimated to be 6.44 eV. This large value confirms the unusual stability of the dianion in the gas phase. We also calculate and plot the wave functions of HOMO and LUMO. Both of these have distributions on the B cage, but show different behavior on the ligands. The HOMO on the CN is more delocalized with π character while the LUMO is localized on N with p character.

Having demonstrated the great stability of $B_{12}(CN)_{12}^{2-}$ originating from the substitution of H by the highly electronegative ligand CN, we now focus on the stability of $CB_{11}(CN)_{12}^{2-}$. To demonstrate the effect of the ligand we begin with a study of the stability of $CB_{11}H_{12}^{2-}$. The binding energy of the second electron (ΔE_2) in $CB_{11}H_{12}^{2-}$ is found to be −3.26 eV. Thus, $CB_{11}H_{12}^{2-}$ is unstable against autodetachment of an electron. This characteristic is expected as the molecule contains one electron more than needed to satisfy the Wade-Mingos electron shell closure rule. Would substitution of H by CN change this scenario? To study this, we optimized the geometries of neutral, monoanionic, and dianionic forms of $CB_{11}(CN)_{12}$. The results are given in Figures 4a–c. After full geometry relaxation we observe that the replacement of B by C (denoted as C_B) reduces the symmetry of the system compared to that of $B_{12}(CN)_{12}$. The neutral $CB_{11}(CN)_{12}$ has a C_s point-group symmetry. The average bond length between C and B is 1.52 Å and that between C and C_B is 1.44 Å. The average C_B–B and B–B bond lengths are found to be 1.75 and 1.81 Å, respectively. When one electron is attached, the $CB_{11}(CN)_{12}^{-}$ has a C_5 point-group symmetry. The binding energy of the added electron, ΔE_1 given by Equation (1) is 8.72 eV (Table 1). This value is much larger than that in the case of $CB_{11}H_{12}$, as it is 5.36 eV. When we add the second electron into the system, we find that $CB_{11}(CN)_{12}^{2-}$ is distorted additionally, around the C_B site and the point-group symmetry reduces to C_1. The average B–B bond length around the C_B site is 1.86 Å, while the average C_B–B bond length on the cage is 1.84 Å. Surprisingly, the binding energy of the second electron $CB_{11}(CN)_{12}^{2-}$ is +1.07 eV. This value means that $CB_{11}(CN)_{12}^{2-}$ is stable against autodetachment of the electron, and is contrary to expectation as $CB_{11}(CN)_{12}^{2-}$,

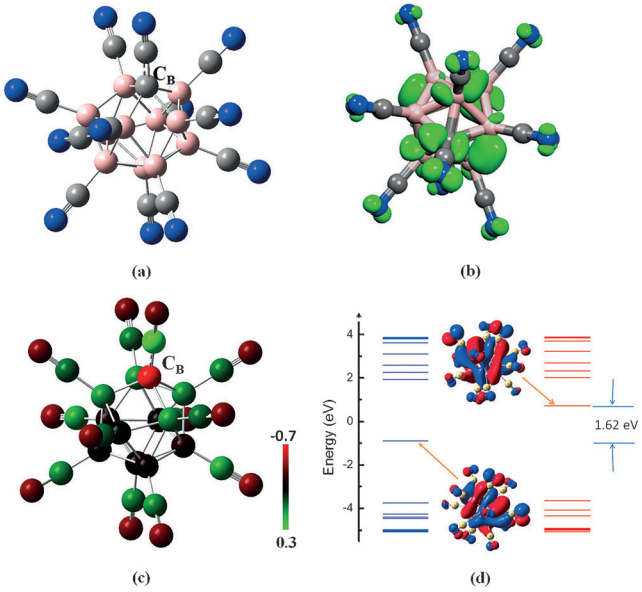

Figure 4. a) Geometric structure, b) spin density, c) NBO charge distribution, and d) energy diagram and frontier orbitals of $CB_{11}(CN)_{12}^{2-}$.

like $CB_{11}H_{12}^{2-}$, contains one more electron than needed to satisfy the Wade-Mingos electron-counting rule. Thus, replacement of H by CN not only increases the magnitude of the electron binding energy, but also stabilizes a multiply charged dianion against its electron shell closure rule. Because of the odd number of total electrons, $CB_{11}(CN)_{12}^{2-}$ has a magnetic moment of 1 μ_B which is distributed over the entire system (Figure 4b).

According to the NBO analysis each B in the neutral $CB_{11}(CN)_{12}$ cage loses 0.08 electrons on the average. The C_B site gains 0.57 electrons while each CN pair receives 0.03 electrons. In $CB_{11}(CN)_{12}^{-}$ each CN pair gains 0.09 electrons on the average, each B atom loses 0.06 electrons, and the charge state of C_B remains almost unchanged. In $CB_{11}(CN)_{12}^{2-}$ the CN ligands also receive most of the charge, whereas the charged state of C_B becomes −0.67, and the B atoms continue to loose electrons (Figure 4c). The high electronegativity of CN ligands is the main reason for the large first and second EA of $CB_{11}(CN)_{12}$. The energy diagram and molecular orbitals of $CB_{11}(CN)_{12}^{2-}$ are shown in Figure 4d. We see that HOMO and LUMO are in spin up and spin down channels, respectively, with a gap of 1.62 eV.

Very recently it was proposed that $CB_{11}H_{12}^{-}$ can work as a high-performance halogen-free electrolyte in lithium ion batteries because of its smaller binding energy with cations (e.g. Li^+ binding energy with $CB_{11}H_{12}^{-}$ is only ≈5.08 eV),[18] relative to those in currently used electrolytes in lithium ion batteries. This theoretical prediction has already been confirmed experimentally in lithium and magnesium ion batteries.[19,20] We note that the binding energy of the cation to the anion depends on the size of the anion. As the anion size increases, the distance between the cation and anion would increase and the binding energy should decrease. Since the diameter of $B_{12}(CN)_{12}^{2-}$ (ca. 8.8 Å) is larger than those of $CB_{11}H_{12}^{-}$ and $B_{12}H_{12}^{2-}$ (ca. 5.8 Å), we expect that the binding

energy of the cations (Li^+ or Mg^{2+}) to be reduced, thus improving the battery performance. To get a quantitative estimate of the cation binding energy, we have optimized the geometries of Li_2X, LiX^-, and MgX, where $X = B_{12}H_{12}$ or $B_{12}(CN)_{12}$, and calculated the energies necessary to remove the first and second lithium ion as well as the magnesium ion,

$$\Delta E_{Li1} = E(Li^+) + E(Li_1X^-) - E(Li_2X), \quad (3)$$

$$\Delta E_{Li2} = E(Li^+) + E(X^{2-}) - E(Li_1X^-), \quad (4)$$

$$\Delta E_{Mg} = E(Mg^{2+}) + E(X^{2-}) - E(MgX). \quad (5)$$

ΔE_{Li1} and ΔE_{Li2} are the dissociation energies when the first and second Li^+ are removed from the stable salt Li_2X. ΔE_{Mg} is the dissociation energy for MgX. The optimized structures of the lithium and magnesium salts are given in Figure 5. For the lithium salts, we find that the Li atoms prefer to adsorb on the center of the islands formed by the three N (or H) atoms on the opposite sites of the cage. Our calculated dissociation energies are summarized in Table 2. ΔE_{Li1} and ΔE_{Li2} for $Li_2B_{12}H_{12}$ are 5.91 and 9.03 eV, respectively. These values are consistent with previous results (5.94 eV and 9.00 eV respectively).[18] These values are both higher than that in the previously proposed $LiCB_{11}H_{12}$,[18] hence $Li_2B_{12}H_{12}$ was judged not to be a good candidate as an electrolyte for a lithium ion battery. As for $Li_2B_{12}(CN)_{12}$, the calculated ΔE_{Li1} and ΔE_{Li2} are 4.66 and 6.83 eV, respectively. These values are significantly lower than those in $Li_2B_{12}H_{12}$ and lie in the range for electrolytes used in current lithium ion batteries.[18] For the magnesium salts, the ΔE_{Mg} for $B_{12}H_{12}$ and $B_{12}(CN)_{12}$ are found to be 21.31 eV and 17.46 eV, respectively. Again $MgB_{12}(CN)_{12}$ would be a better candidate as an electrolyte for a magnesium ion battery than $MgB_{12}H_{12}$.

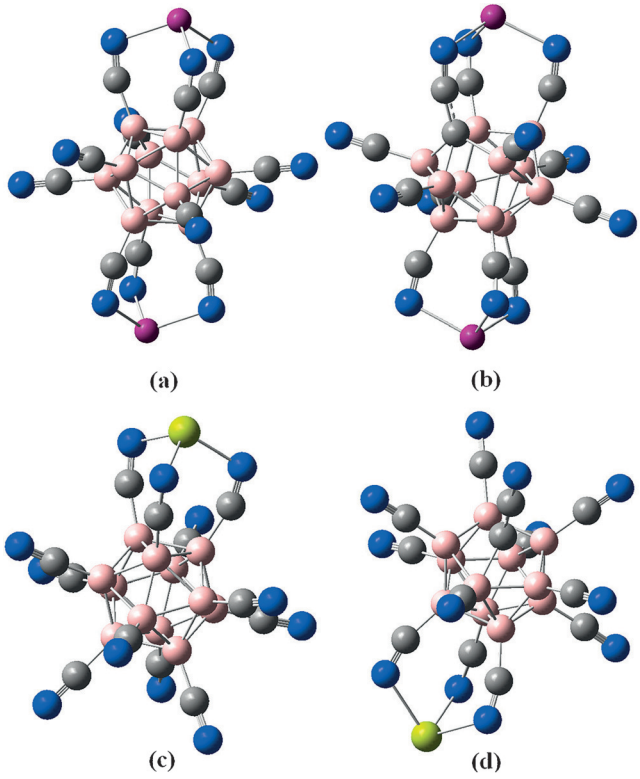

Figure 5. Optimized geometries of a) $Li_2B_{12}(CN)_{12}$, b) $Li_2CB_{11}(CN)_{12}$, c) $MgB_{12}(CN)_{12}$, and d) $MgCB_{11}(CN)_{12}$.

Table 2: Dissociation energies in lithium salts (ΔE_{Li1}, ΔE_{Li2}) and in magnesium salts (ΔE_{Mg}).

	ΔE_{Li1} (eV)	ΔE_{Li2} (eV)		ΔE_{Mg} (eV)
$Li_2B_{12}H_{12}$	5.91	9.03	$MgB_{12}H_{12}$	21.31
$Li_2B_{12}(CN)_{12}$	4.66	6.83	$MgB_{12}(CN)_{12}$	17.46
$LiCB_{11}(CN)_{12}$	4.09		$MgCB_{11}(CN)_{12}$	18.30
$Li_2CB_{11}(CN)_{12}$	4.67	6.89		

We have also explored the potential of $CB_{11}(CN)_{12}$ as an electrolyte. As pointed out in the above, recently $CB_{11}H_{12}^-$ was predicted to be a good halogen-free electrolyte. To examine if $CB_{11}(CN)_{12}^-$ may be a better candidate for an electrolyte rather than $CB_{11}H_{12}^-$, we calculated the binding energy of Li in the $LiCB_{11}(CN)_{12}$ salt. This binding energy, namely 4.09 eV, is smaller than that in $LiCB_{11}H_{12}$ (5.08 eV), and implies that it will be easier to detach Li^+ from $LiCB_{11}(CN)_{12}$ than from $LiCB_{11}H_{12}$. The other advantage of $CB_{11}(CN)_{12}$ is that it is stable also as a dianion. This data means that electrolytes such as $Li_2CB_{11}(CN)_{12}$ and $MgCB_{11}(CN)_{12}$ are also possible. The advantage of the former is that current density can be higher than that in $LiCB_{11}H_{12}$. The calculated binding energy of the two Li atoms in $Li_2CB_{11}(CN)_{12}$ are $\Delta E_{Li1} = 4.67$ eV and $\Delta E_{Li2} = 6.89$ eV, and they are also significantly lower than those in $Li_2B_{12}H_{12}$. The binding energy of Mg^{2+} in $MgCB_{11}(CN)_{12}$ is 18.30 eV, which is also significantly lower than that in $MgB_{12}H_{12}$ (21.31 eV) and comparable to that in $MgB_{12}(CN)_{12}$ (17.46 eV).

In summary, we show that ligand engineering can lead to some remarkable results. The *closo*-borane $B_{12}H_{12}^{2-}$, known for its stability as a dianion in the gas phase can be made unusually more stable by replacing H with CN. For example, the binding energy of the second electron in $B_{12}(CN)_{12}^{2-}$ is 5.3 eV, which is about six times larger than that in $B_{12}H_{12}^{2-}$. To our knowledge, no other molecule, of this size, exists that is more stable as a dianion than $B_{12}(CN)_{12}^{2-}$. Equally important is our observation that $CB_{11}(CN)_{12}^{2-}$ is also stable with the second electron bound by 1.07 eV. This observation was not expected as $CB_{11}(CN)_{12}^{2-}$ contains one more electron than necessary to satisfy the Wade-Mingos electron shell closure rule. In chemistry, several electron-counting rules, such as the octet rule, 18-electron rule, aromatic rule, and Wade-Mingos rule exist and account for the stability of many molecules. These rules are routinely used to design both stable and reactive species. Our studies show that ligand engineering is another option which can yield similar results. Application of these unusually stable multiply charged anions in the design and synthesis of halogen-free electrolytes in either lithium, sodium, or magnesium ion batteries is also presented. We show that $LiCB_{11}(CN)_{12}$, $Li_2CB_{11}(CN)_{12}$, $Li_2B_{12}(CN)_{12}$, $MgB_{12}(CN)_{12}$, and $MgCB_{11}(CN)_{12}$ possess better properties as electrolytes in metal ion batteries than those where CN molecules are replaced by H atoms. Our results are based on density-functional theory whose predictive power has already been proven experimentally. We hope that these results will stimulate the synthesis of $B_{12}(CN)_{12}$ and experimental study

of its unusual properties. We note that experimental studies of $B_{12}X_{12}$ (X = F, Cl, Br, and I) have already showcased their remarkable properties.[21]

Experimental Section

Our results are obtained using first-principles calculations based on density-functional theory (DFT). We used hybrid functional B3LYP for exchange-correlation potential[22,23] and the 6-31 + G(d,p) basis set for all the atoms embedded in the Gaussian 03 code.[24] All geometries were fully optimized without any symmetry constraint. The total energies and forces were converged to 2.7×10^{-5} eV and 0.02 eV Å^{-1}, respectively. Frequency analyses were performed to ensure that the structure belongs to a minimum on the potential energy surface. Charge analysis was carried out using the natural bond orbital (NBO) method.[25,26] To check the sensitivity of our results to numerical procedure we have repeated our calculations using the Vienna ab initio simulation package (VASP)[27] and HSE06 form hybrid functional for exchange-correlation potential.[28] Computations of the geometries and total energies were carried out using a plane-wave basis set with energy cutoff of 400 eV. Vacuum space of 15 Å in *x*, *y*, and *z* directions was applied and the reciprocal space was represented by the Γ point. The results obtained using these two different methods agree with each other, giving us confidence in the numerical results and the predictive power of our approach.

Acknowledgements

The authors thank Dr. Jonas Warneke for a critical reading of the manuscript and helpful discussions. This work is supported in part by the Fundamental Research Funds for Central University (2013JBM102), the U. S. Department of Energy, Office of Basic Energy Sciences, Division of Materials Sciences and Engineering under Award # DE-FG02-96ER45579 and # DE-FG02-11ER46827, and by CIT CRCF. Hongmin Zhao acknowledges the China Scholarship Council (CSC) for sponsoring her visit to Virginia Commonwealth University (VCU) where this work was conducted. Resources of the National Energy Research Scientific Computing Center supported by the Office of Science of the U.S. Department of Energy under Contract No. DE-AC02-05CH11231 is also acknowledged.

Keywords: cluster compounds · cyanoborate cluster · electronic structure · ion battery · ligand effects

How to cite: *Angew. Chem. Int. Ed.* **2016**, *55*, 3704–3708
Angew. Chem. **2016**, *128*, 3768–3772

[1] E. Zintl, J. Goubeau, W. Dullenkopf, *Z. Phys. Chem. Abt. A* **1931**, *154*, 1–46.
[2] E. Zintl, H. Kaiser, *Z. Anorg. Allg. Chem.* **1933**, *211*, 113–131.
[3] G. L. Gutsev, A. I. Boldyrev, *J. Phys. Chem.* **1990**, *94*, 2256–2259.
[4] A. Dreuw, L. S. Cederbaum, *Chem. Rev.* **2002**, *102*, 181–200.
[5] A. I. Boldyrev, M. Gutowski, J. Simons, *Acc. Chem. Res.* **1996**, *29*, 497–502.
[6] S. Li, M. Willis, P. Jena, *J. Phys. Chem. C* **2010**, *114*, 16849–16854.
[7] M. L. McKee, Z. X. Wang, P. v. R. Schleyer, *J. Am. Chem. Soc.* **2000**, *122*, 4781–4793.
[8] K. Wade, *J. Chem. Soc. D* **1971**, 792–793.
[9] K. Wade, *Adv. Inorg. Chem. Radiochem.* **1976**, *18*, 1–66.
[10] D. M. P. Mingos, *Acc. Chem. Res.* **1984**, *17*, 311–319.
[11] D. M. P. Mingos, R. L. Johnston, *Struct. Bonding (Berlin)* **1987**, *68*, 29–87.
[12] S. Giri, B. Z. Child, J. Zhou, P. Jena, *RSC Adv.* **2015**, *5*, 44003–44008.
[13] A. I. Boldyrev, J. Simons, *J. Chem. Phys.* **1992**, *97*, 2826–2827.
[14] B. Z. Child, S. Giri, S. Gronert, P. Jena, *Chem. Eur. J.* **2014**, *20*, 4736–4745.
[15] R. T. Boeré, J. Derendorf, C. Jenne, S. Kacprzak, M. Keßler, R. Riebau, S. Riedel, T. L. Roemmele, M. Rühle, H. Scherer, T. Vent-Schmidt, J. Warneke, S. Weber, *Chem. Eur. J.* **2014**, *20*, 4447–4459.
[16] B. Pathak, D. Samanta, R. Ahuja, P. Jena, *ChemPhysChem* **2011**, *12*, 2423–2428.
[17] S. Nosé, *J. Chem. Phys.* **1984**, *81*, 511–519.
[18] S. Giri, S. Behera, P. Jena, *Angew. Chem. Int. Ed.* **2014**, *53*, 13916–13919; *Angew. Chem.* **2014**, *126*, 14136–14139.
[19] Q. Tutusaus, R. Mohtadi, T. S. Arthur, F. Mizuno, E. G. Nelson, Y. V. Sevryugina, *Angew. Chem. Int. Ed.* **2015**, *54*, 7900–7904; *Angew. Chem.* **2015**, *127*, 8011–8015.
[20] W. S. Tang, A. Unemoto, W. Zhou, V. Stavila, M. Matsuo, H. Wu, S. Orimo, T. J. Udovic, *Energy Environ. Sci.* **2015**, *8*, 3637–3645.
[21] J. Warneke, T. Dulcks, C. Knapp, D. Gabel, *Phys. Chem. Chem. Phys.* **2011**, *13*, 5712–5721.
[22] A. D. Becke, *J. Chem. Phys.* **1993**, *98*, 5648–5652.
[23] C. Lee, W. Yang, R. G. Parr, *Phys. Rev. B* **1988**, *37*, 785–789.
[24] M. J. Frisch, G. W. Trucks, H. B. Schlegel, G. E. Scuseria, M. A. Robb, J. R. Cheeseman, J. A. Montgomery, Jr., T. Vreven, K. N. Kudin, J. C. Burant, J. M. Millam, S. S. Iyengar, J. Tomasi, V. Barone, B. Mennucci, M. Cossi, G. Scalmani, N. Rega, G. A. Petersson, H. Nakatsuji, M.Hada, M. Ehara, K. Toyota, R. Fukuda, J. Hasegawa, M. Ishida, T. Nakajima, Y. Honda, O. Kitao, H. Nakai, M. Klene, X. Li, J. E. Knox, H. P. Hratchian, J. B. Cross, V. Bakken, C. Adamo, J. Jaramillo, R. Gomperts, R. E. Stratmann, O. Yazyev, A. J. Austin, R. Cammi, C. Pomelli, J. W. Ochterski, P. Y. Ayala, K. Morokuma, G. A. Voth, P. Salvador, J. J. Dannenberg, V. G. Zakrzewski, S. Dapprich, A. D. Daniels, M. C. Strain, O. Farkas, D. K. Malick, A. D. Rabuck, K. Raghavachari, J. B. Foresman, J. V. Ortiz, Q. Cui, A. G. Baboul, S. Clifford, J. Cioslowski, B. B. Stefanov, G. Liu, A. Liashenko, P. Piskorz, I. Komaromi, R. L. Martin, D. J. Fox, T. Keith, M. A. Al-Laham, C. Y. Peng, A. Nanayakkara, M. Challacombe, P. M. W. Gill, B. Johnson, W.Chen, M. W. Wong, C. Gonzalez, J. A. Pople, Gaussian 03, RevisionD.02, Gaussian, Inc., Wallingford CT, **2004**.
[25] A. E. Reed, L. A. Curtiss, F. Weinhold, *Chem. Rev.* **1988**, *88*, 899–926.
[26] E. D. Glendening, A. E. Reed, J. E. Carpenter, F. Weinhold, NBO Version 3.1.
[27] G. Kresse, J. Furthmuller, *Phys. Rev. B* **1996**, *54*, 11169–11186.
[28] a) J. Heyd, G. E. Scuseria, M. Ernzerhof, *J. Chem. Phys.* **2003**, *118*, 8207–8215; b) J. Heyd, G. E. Scuseria, M. Ernzerhof, *J. Chem. Phys.* **2006**, *124*, 219906–1.

Received: January 10, 2016
Published online: February 16, 2016

